Quantifying Loss of Control Envelopes via Robust Tracking Analysis

Harald Pfifer*

University of Nottingham, NG7 2RD

Raghu Venkataraman † and Peter Seiler ‡

University of Minnesota, Minneapolis, MN 55455

Nomenclature

e	control error	
q	pitch rate	$[^\circ/s]$
r	reference command	
u	plant input	
y	plant output	
x	state vector	
A, B, C, D	state space matrices	
$F_u(.,.)$	upper fractional transformation	
G_ρ	linear parameter varying plant	
K_ρ	gain scheduled controller	
W	weighting filter	
S	sensitivity function	
V	airspeed	[m/s]
$\mathcal{P}$	set defining the permissible flight envelope	
$\mathbb{R}$	set of real numbers	
$\mathbb{S}^n$	set of symmetric matrices of size n	
$\mathcal{T}$	set of admissible parameter trajectories	
α	angle of attack	$[^\circ]$

*Assistant Professor, Department of Mechanical Engineering, University of Nottingham, harald.pfifer@nottingham.ac.uk

†Graduate Student, Aerospace Engineering and Mechanics Department, University of Minnesota, venka085@umn.edu

‡Associate Professor, Aerospace Engineering and Mechanics Department, University of Minnesota, seile017@umn.edu

Δ	uncertainty set	
ρ	scheduling parameter	
ω	frequency	[rad/s]

I. Introduction

This paper proposes the usage of robust tracking as a quantification of the permissible flight envelope. It is meant to compliment the work in [1]. In [1], different permissible envelopes are defined based on physical characteristics of an aircraft, e.g. angle of attack and sideslip angle. The results of [1] are summarized in Section II.A. Based on flight data it was established that these envelopes are indicative for loss of control (LOC). The main contribution of this paper is to extend this idea by quantifying the permissible flight envelope. A key motivation for proposing techniques to estimate a priori the permissible flight envelope is the lack of flight data for LOC [2]. Hence, it is important to have an estimation tool that provides a good envelope prediction without resorting to extensive flight data.

Robust tracking performance is proposed as a metric for this quantification. While tracking is not meant as a comprehensive characteristics to define LOC, it does play a major role in qualitative definitions that are used in literature, e.g. in [1]. The proposed metric can be readily evaluated on several levels of model complexity, as is described in Section II.B. In the simplest case, it amounts to a norm calculation of a linear time invariant system that represents an aircraft at a fixed flight condition. It can be extended to include uncertainties in the aircraft model and/or account for time-varying trajectories in the flight envelope. Both are considered important aspects for LOC events. It was shown in [2] that model quality outside the nominal flight envelope is usually less evolved. This can be mainly contributed to the previously mentioned lack of flight data for these off-nominal conditions. Therefore, adding uncertainty in the flight dynamics models for quantitative LOC analysis is critical. Additionally, LOC events are usually characterized by large motion and deviation of trim conditions. Disregarding these changing dynamics may lead to an overly optimistic quantification of the flight envelope. Computationally tractable algorithm are available to evaluate the proposed metric. These build on the work of [3–5] and are summarized in Section III. It shall be emphasized that the control system plays an integral role in the achievable tracking performance. Hence, the proposed metric does not purely depend on the aircraft dynamics but is also influenced by the performance of the chosen flight controller.

Traditionally LOC studies are based on linear analysis supplemented with Monte Carlo simulations of the full nonlinear aircraft models. Recently LOC research focused on advanced linear and nonlinear methods to analyze the robust stability and performance of nonlinear systems. An overview of these advances is, for instance, given in [6] and [2]. These approaches can vary vastly on the level of complexity. On the low complexity side, the attainable steady state solutions are examined to estimate flight envelope [7]. On the other end of the spectrum the nonlinear aircraft dynamics is analysed directly based on bifurcation [8]. Reachability and region of attraction analysis is often employed in literature [9–12]. These methods can be computationally very demanding and, in general, rely on solving Hamilton-

Jacobi equations [13]. The approach taken in this paper is based on simpler linear or linear parameter varying system descriptions and can treat nonlinearities in form of uncertainty. However, it still deals with the dynamic behavior of the aircraft and does not restrict itself to the steady state solution. The proposed approach is computationally not very demanding an it is anticipated that it can be included in online envelope estimation tools, e.g. the ones proposed in [14]. Note that the linear parameter varying framework has been widely used in literature to study high performance aircraft even beyond the linear flight regime, see for example [15, 16]. The framework has also been applied in [17] to analyse control upset prevention and recovery.

II. Quantitative Loss of Control

A. Summary of Existing Quantitative LOC Metrics

A report by the Joint Safety Analysis Team, itself chartered by the Commercial Aviation Safety Team, defines LOC to include "significant, unintended departure of the aircraft from controlled flight, the operational flight envelope, or usual flight attitudes, including ground events" [18]. For further study it is important to have a formal definition which includes measurable, quantitative LOC metrics. This is precisely the aim of [1] where key flight dynamics parameters are identified for predicting LOC. These parameters were grouped into five permissible flight envelopes that characterize LOC. Flight data was used to tune the size of the flight envelopes and validate their importance in terms of LOC. The remainder of this section briefly summarizes the metrics proposed in [1] as this will motivate the use of robust tracking as proposed in Section B.

The flight envelopes proposed in [1] are called Quantitative Loss of Control Criteria (QLC). These envelopes are chosen to broadly capture qualitative features that define LOC. The qualitative LOC features, taken directly from [1], correspond to aircraft dynamics that are:

"
- outside the normal operating flight envelopes
- not predictably altered by pilot control inputs
- characterized by nonlinear effects, such as kinematic/inertial coupling, disproportionately large responses to small state variable changes, or oscillatory/divergent behavior
- likely to result in high angular rates and displacements
- characterized by the inability to maintain heading, altitude, and wings-level flight"

Five flight envelopes are specified to capture these qualitative features. First, the adverse aerodynamic envelope bounds the angle of attack and sideslip angle. It considers both stall at high angle of attack as well as sideslip induced roll. Second, the unusual attitude envelope is defined by the bank and pitch angle. This envelope is an indicator for stall, excessive roll and nose high/nose low unusual attitude. Violating the adverse aerodynamic envelope will frequently also violate the unusual attitude envelope. However, the converse is not necessarily true. The next envelope, denoted

structural integrity envelope in [1], maps the airspeed against the load factor. This envelope considers the limits of the structural design of the aircraft. The final two envelopes, namely the dynamic pitch control and dynamic roll control, are used to assess the consistency between the pilot command and aircraft response in the longitudinal and lateral motion respectively. Violations of these envelopes are indicators for dynamic events such as pilot induced oscillations or wake vortex encounters. Note that while these envelopes were sufficient in analyzing the available flight data in [1], the authors indicate that the list is not meant to be comprehensive. Specifically, the envelopes should account for different aircraft configurations, e.g. different masses, center of gravity positions or flap configurations.

The QLC proposed by Wilborn and Foster provide a useful starting point for analysis. A key issue is that LOC events are extremely rare and hence there is limited flight data for such events. Moreover, experimental LOC flight tests are restricted by safety regulations [2]. Hence additional data is mainly available via scaled remote-controlled aircraft, e.g. NASA's AirSTAR infrastructure [19]. This lack of flight data limits the validation that can be done on the QLC proposed in [1]. The lack of flight data also limits the *design* of the flight envelopes that constitute the QLC. In particular, the LOC flight envelopes are defined by various design parameters. For example, the unusual attitude envelope is parameterized by maximum magnitudes for the bank and pitch angles. Typical (industry accepted) values are specified in [1] for the maximum bank and pitch angles. However, such parameters could be selected specifically for a given aircraft. More importantly, the parameters that define the LOC flight envelopes should be selected based on the aircraft configuration (as noted above). The limited LOC flight data is insufficient for this purpose as a typical commercial aircraft has many possible configurations. In summary, it would be useful to have a means to select the LOC flight envelopes based on the characteristics of a specific aircraft in a specific configuration.

The description of the flight envelope so far only considered the nominal, i.e. the undamaged, operation of the aircraft. Besides different aircraft configurations, fault scenarios have a big impact on the LOC flight envelope. While this paper does not explicitly considers fault scenarios, the approach proposed in the following section can be handily adapted to cover these situations. It requires the availability of a model description of the damaged aircraft. This description can be either generated offline based on a set of scenarios or onboard in conjunction with an online parameter estimation algorithm as described in [20].

B. Proposed Quantitative LOC Metric: Robust Tracking

The basic premise of this paper is that a robust tracking analysis can be used to determine the permissible flight envelope. As summarized previously, the QLC in [1] consists of five flight envelopes specified as rectangles or, more generally, polytopes. The permissible flight envelope computed via tracking performance can be used to define the boundaries of these proposed LOC envelopes. The motivation for this premise is that LOC is qualitatively characterized by inability to properly track commands. For example, bullets 2 and 5 of the qualitative LOC characteristics defined in [1] (and repeated in Section A above) state that LOC corresponds to motion that is "not predictably altered by pilot control inputs" and is "characterized by the inability to maintain heading, altitude, and wings-level flight".

These are both controls-related features.

The proposed approach is to analyze the robust tracking performance of the aircraft at various points of the flight envelope. Roughly, robust tracking performance refers to the largest gain from reference commands to tracking error in the presence of model uncertainty. Additional details on the proposed robust tracking analysis are provided below. A large degradation in tracking performance at some flight condition is a qualitative feature of LOC and hence this flight condition should not be included in the permissible flight envelope. The proposed robust tracking analysis complements the work in [1] as it provides a means to define the boundaries of the LOC flight envelopes for various aircraft and configurations. There is also the potential to use robust tracking analysis as a real-time indicator for LOC. This would build on the Run-time Observation-based Margin Estimation (ROME) tool described in [14]. ROME is an on-line tool to monitor stability margins in flight. Extending the ROME tool to include monitoring of robust tracking performance would be useful as degradations in tracking performance can, in some cases, occur prior to degradations in stability margins. Finally, we note that some of the envelopes given in [1] can be analyzed purely from an aerodynamics and structural dynamics perspective. The structural integrity envelope is one example. The proposed robust tracking analysis is not suitable for these envelopes. This paper instead focuses only on features of the LOC envelope that are correlated with the performance of the control system. The remainder of the section describes the proposed analysis in more detail.

1. Nominal LTI Analysis

Consider the classical feedback diagram shown in Figure 1 consisting of a plant and controller. Initially assume, for simplicity, that the plant and controller are single input, single output. The parameter ρ specifies an operating point in the flight envelope, e.g. an angle of attack and sideslip angle in the adverse aerodynamic envelope. The plant G_ρ represents the linearized aircraft dynamics at the operating point ρ. Flight control laws are typically gain-scheduled and K_ρ denotes the (linear) control law scheduled for operating point ρ. Both the plant and controller are linear, time invariant (LTI) systems at a fixed operating condition (constant ρ). The basic tracking objective is for the output y to follow a reference command r. Equivalently the tracking objective is to keep the error $\tilde{e}$ small despite reference commands and other effects, e.g. sensor noise and disturbances such as wind gusts. Note that disturbances would be modelled as additional inputs in the interconnection Figure 1. For instance, sensor noise can be directly added as an external input to the measurement signal y.

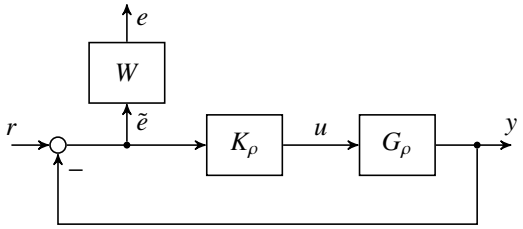

Figure 1. Closed Loop Tracking Performance

In this paper we follow a robust control methodology and use a weighted norm to measure the tracking performance [21]. To be concrete, the sensitivity transfer function from r to error $\tilde{e}$ at operating point ρ is $S_\rho(s) := \frac{1}{1+G_\rho(s)K_\rho(s)}$. A typical performance objective can be specified as $|S(j\omega)| \leq |B(j\omega)|$ where the bound $B(s)$ is defined as follows:

$$B(s) := \frac{2s + \epsilon\omega_B}{s + \omega_B} \tag{1}$$

This bound specifies a low frequency tracking objective of $|S_\rho(j\omega)| \leq \epsilon$ and an approximate bandwidth of ω_B. In addition, the bound specifies that $\|S_\rho\|_\infty \leq 2$ which ensures reasonable gain/phase margins. The performance objective can be rewritten as $\|WS_\rho\|_\infty \leq 1$ where the weight is given by:

$$W(s) := B(s)^{-1} = \frac{s + \omega_B}{2s + \epsilon\omega_B} \tag{2}$$

The desired performance is thus normalized to one, i.e. a properly designed controller should satisfy $\|WS_\rho\|_\infty \leq 1$ at all operating points ρ in the nominal flight envelope. This weight is shown in Figure 1 as a filter with the true tracking error $\tilde{e}$ as input. The performance objective can be interpreted as the weighted induced L_2 gain from reference r to weighted error e. We expect the tracking performance to degrade if/when the aircraft moves out of the nominal flight envelope. This weighted tracking performance can used to define a permissible flight envelope. The permissible flight envelope for a given level of performance degradation $\kappa > 1$ is defined as follows.

Definition 1. The *nominal LTI permissible flight envelope* is the largest polytope $\mathcal{P}$ such that $\|WS_\rho\|_\infty \leq \kappa$ for all fixed operating conditions $\rho \in \mathcal{P}$.

By definition, tracking performance in the permissible flight envelope is within a small factor κ of the desired (weighted) performance. Larger performance degradation is observed outside this permissible envelope and hence this may indicate LOC. In this approach κ is a single parameter that defines the boundary between acceptable and unacceptable tracking performance. We propose a value of $\kappa = 1.3$ and any available flight data can be used to further refine this parameter.

Definition 1 aims to guarantee that the aircraft exhibits a predictable response to pilot inputs within the permissible flight envelope. The definition includes the qualifiers "nominal" and "LTI". The use of LTI indicates that the analysis is performed for a single fixed operating point ρ. Hence the plant and gain-scheduled controller are both assumed to be LTI in this definition. The use of "nominal" indicates that no model uncertainty is considered. Removing both of these restrictions leads to a more general robust tracking analysis as defined below. Finally, this section described the basic approach for a classical SISO control loop. A more realistic control architecture for commercial aircraft would be more complicated, including multiple inputs, multiple-outputs, inner-loop rate feedbacks, etc. A similar permissible envelope can be defined even for more complex control architectures. This extension requires the overall performance objective to be specified as a single weighted norm as is commonly used in H_∞-controller synthesis [21].

2. *Robust and LPV Analysis*

This section describes two important extensions to the nominal LTI permissible flight envelope. First, Figure 2 shows a modification of the classical loop to include plant uncertainty. This plant uncertainty can arise due to parametric uncertainty (e.g. in the aerodynamic coefficients) or unmodeled dynamics (e.g. flexible aircraft dynamics or actuator uncertainty). These are the types of uncertainties considered in the typical robust control formulation [22]. Key nonlinearities such as actuator saturation and rate limits can also be included using the integral quadratic constraint (IQC) framework [23]. In general, this leads to a set of possible uncertainties $\mathbf{\Delta}$ and hence a set of possible plant models $\{F_u(G_\rho, \Delta) \ : \ \Delta \in \mathbf{\Delta}\}$. Here $F_u(G_\rho, \Delta)$ denotes the uncertain plant from u to y formed by wrapping Δ around the top channels of G_ρ as shown in Figure 2. Each uncertain plant thus yields a potentially different sensitivity function $S_\rho(\Delta)$ at the (constant) operating ρ. A robust tracking formulation that considers the effects of these uncertainties is formally defined as follows:

Definition 2. The *robust LTI permissible flight envelope* is the largest polytope $\mathcal{P}$ such that $\|WS_\rho(\Delta)\|_\infty \leq \kappa$ for all uncertainties $\Delta \in \mathbf{\Delta}$ and all fixed operating conditions $\rho \in \mathcal{P}$.

As noted in [1], loss of control events are characterized by aircraft dynamics that are "outside the normal operating flight envelopes". Since flight data to validate models for these off-nominal conditions is limited, dynamic models likely have higher levels of uncertainty during LOC events. Hence it is important to consider the effect of model uncertainty when defining the permissible flight envelope. Definition 2 addresses this issue. In addition, the use of IQCs has the potential to incorporate nonlinear effects in the analysis. This partially addresses one of the qualitative LOC features mentioned in [1] (and repeated as bullet 3 in Section A).

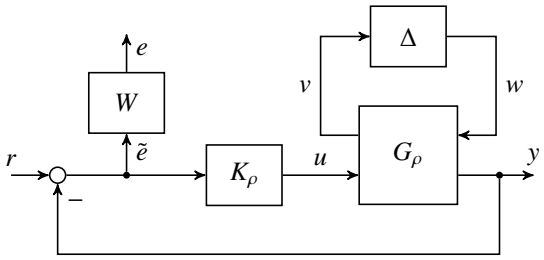

Figure 2. Robust Closed-Loop Tracking Performance

The second important extension to the permissible flight envelope is to consider time-varying operating conditions. Definitions 1 and 2 are based on LTI analyses at fixed operating points throughout the envelope. This is potentially overly-optimistic as aircraft LOC events are characterized by large motions and deviations from equilibrium conditions. Hence it is useful to quantify the impact of time-varying operating conditions, i.e. $\rho(t)$ varies in time. In this case both the plant dynamics G_ρ and the gain-scheduled controller K_ρ should be modeled by linear parameter varying (LPV) systems.

Linear Parameter Varying (LPV) systems are a class of linear systems whose state space matrices depend on a time-

varying parameter vector $\rho : \mathbb{R} \to \mathbb{R}^{n_\rho}$. The parameter ρ is assumed to be a continuously differentiable function of time and admissible trajectories are restricted, based on physical considerations, to a known compact subset. In addition, the parameter rates of variation $\dot{\rho}(t)$ are assumed to lie within a known hyperrectangle $\dot{\mathcal{P}}$. The set of admissible parameter trajectories is defined by $\mathcal{T} := \left\{\rho : \mathbb{R}^+ \to \mathbb{R}^{n_\rho} \ : \ \rho \in C^1,\ \rho(t) \in \mathcal{P} \text{ and } \dot{\rho}(t) \in \dot{\mathcal{P}}\ \forall t \geq 0\right\}$. The state-space matrices of an LPV system are continuous functions of the parameter ρ, e.g. $A_G : \mathcal{P} \to \mathbb{R}^{n_x \times n_x}$. Define the LPV system G_ρ with input r and outputs e as:

$$\begin{aligned} \dot{x}_G(t) &= A_G(\rho(t))x_G(t) + B_G(\rho(t))r(t) \\ e(t) &= C_G(\rho(t))x_G(t) + D_G(\rho(t))r(t) \end{aligned} \tag{3}$$

The state matrices at time t depend on the parameter vector at time t. The explicit dependence on t is occasionally suppressed in the paper to shorten the notation. The closed-loop sensitivity $S_\rho(\Delta)$ is time-varying and hence does not have a valid frequency response. It is more appropriate to denote the weighted, induced L_2 gain as $\|WS_\rho(\Delta)\|_{2\to 2}$. A robust tracking formulation that accounts for the time-varying operating condition is formally defined as follows:

Definition 3. The *robust LPV permissible flight envelope* is the largest polytope $\mathcal{P}$ such that $\|WS_\rho(\Delta)\|_{2\to 2} \leq \kappa$ for all uncertainties $\Delta \in \mathbf{\Delta}$ and all rate-bounded, time-varying operating trajectories $\rho \in \mathcal{T}$.

III. Computational Approach

This section outlines the numerical methods required to calculate the tracking performance measures used in the various definitions of permissible flight envelopes. In the nominal linear time invariant case, these are standard methods which are readily available, e.g. in Matlab. Tools for computing the more advanced robust and linear parameter varying metrics are available through the Robust Control Toolbox [24] and LPVTools [25, 26], respectively.

A. Nominal and Robust LTI Analysis

Fast algorithm are available to compute the L_2 gain of a nominal LTI system [3, 27]. These are based on a simple bisection algorithm that evaluates the eigenvalues of a related Hamiltonian matrix. In Matlab this bisection algorithm is implemented in the `norm` command. The worst-case L_2 gain is computed using the Matlab Robust Control Toolbox command `wcgain` [24]. The `wcgain` command computes upper and lower bounds on the largest L_2 gain of a known LTI system interconnected with LTI uncertainty. These type of uncertainties are commonly used in the robust control field. They can handle real parametric uncertainties, such as uncertainties in the center of gravity position or more generic dynamic uncertainties, e.g. disk margin constraints. The computations are variations of those used for the structured singular value (μ) and details are provided in [4]. The approach can be extended to incorporate nonlinear effects by resorting to the IQC framework as introduced in [28]. The LTI analysis is performed over a grid of fixed values of the scheduling parameter ρ. The permissible flight envelope is defined by the grid points at which the tracking

performance is less than κ. A bisection algorithm over ρ can be employed to efficiently search for a more accurate boundary of the flight envelope.

B. Nominal Linear Parameter Varying Analysis

In [29] a sufficient condition to upper bound the induced L_2 gain of an LPV system is stated. The sufficient condition uses a quadratic storage function that is defined using a parameter-dependent matrix $P : \mathcal{P} \to \mathbb{S}^{n_x}$. It is assumed that P is a continuously differentiable function of the parameter ρ. In order to shorten the notation, a differential operator $\partial P : \mathcal{P} \times \dot{\mathcal{P}} \to \mathbb{S}^{n_x}$ is introduced as in [30]. ∂P is defined as $\partial P(p, q) := \sum_{i=1}^{n_\rho} \frac{\partial P(p)}{\partial p_i} q_i$. The next theorem states the condition provided in [29] to bound the L_2 gain of an LPV system.

Theorem 1. ([29]): An LPV system G_ρ as defined by Equation (3) is exponentially stable and $\|G_\rho\| < \gamma$ if there exists a continuously differentiable $P : \mathcal{P} \to \mathbb{S}^{n_x}$, such that $\forall (\rho, \dot{\rho}) \in \mathcal{P} \times \dot{\mathcal{P}}$

$$P(\rho) > 0, \tag{4}$$

$$\begin{bmatrix} P(\rho)A_G(\rho) + A_G(\rho)^T P(\rho) + \partial P(\rho, \dot{\rho}) & P(\rho)B_G(\rho) \\ B_G^T(\rho)P(\rho) & -I \end{bmatrix} + \frac{1}{\gamma^2} \begin{bmatrix} C_G(\rho)^T \\ D_G(\rho)^T \end{bmatrix} \begin{bmatrix} C_G(\rho) & D_G(\rho) \end{bmatrix} < 0. \tag{5}$$

Proof. The proof is based on the existence of a quadratic storage function $V(x, \rho) := x^T P(\rho) x$ that satisfies a dissipation inequality. Details are given in [29]. □

Two details must be considered in order to turn this theoretical result into a useful numerical algorithm. First, the conditions Equation (4) and Equation (5) are parameter-dependent linear matrix inequalities (LMIs) that must be satisfied for all possible $(\rho, \dot{\rho}) \in \mathcal{P} \times \dot{\mathcal{P}}$. Thus Equation (4) and Equation (5) represent an infinite collection of LMI constraints. Since $\dot{\rho}$ enters only affinely into the LMI and the set $\dot{\mathcal{P}}$ is a polytope, it is sufficient to check the LMI on the vertices of $\dot{\mathcal{P}}$. On the other hand, ρ can enter Equation (5) nonlinearly through the state matrices and the set $\mathcal{P}$ need not be convex. A remedy to this problem, which works in many practical examples, is to approximate the set $\mathcal{P}$ by a finite set $\mathcal{P}_{grid} \subset \mathcal{P}$. Specifically, the finite set $\mathcal{P}_{grid} := \{\rho^{(k)}\}_{k=1}^N$ represents a grid of points over the set $\mathcal{P}$. The conditions Equation (4) and Equation (5) are enforced only on these grid points leading to a finite dimensional semidefinite program. Note that the gridding approach is only an approximation for the parameter-dependent LMI conditions in Theorem 1. Hence, no rigorous performance guarantees are provided by this gridding approach and special care must be taken when drawing conclusions. A pragmatic implementation of this approach is as follows: Enforce the LMI conditions on a "coarse" grid consisting of a small number of points in order to reduce computation time. The resulting solution can then be checked on a "dense" grid of many points to ensure the accuracy of the solution.

The second detail is that the main decision variable in conditions Equation (4) and Equation (5) is the function $P(\rho)$.

$P(\rho)$ must be restricted to a finite dimensional subspace in order to avoid an infinite dimensional space for the decision variable. A common practice [29], [31] is to restrict the storage function variable $P(\rho)$ to be a linear combination of basis functions $P(\rho) = \sum_{i=1}^{N_b} g_i(\rho) P_i$, where $g_i : \mathbb{R}^{n_\rho} \to \mathbb{R}$ are user-specified basis functions ($i = 1, \ldots, N_b$) and the matrix coefficients $P_i \in \mathcal{S}^{n_x}$ are the decision variables in the optimization.

C. Robust Linear Parameter Varying Analysis

In [5], a worst-case gain condition for an interconnection of a linear parameter varying (LPV) system and an uncertain or nonlinear element. The input/output behavior of the nonlinear/uncertain block is described by an integral quadratic constraint (IQC). A dissipation inequality is proposed in [5] to compute an upper bound for this gain. This condition is a generalization of the well-known Bounded Real Lemma type result for LPV systems given in Theorem 1.

1. Integral Quadratic Constraints

This section describes IQCs for a bounded, causal operator Δ with the input/output behavior described by $w = \Delta(v)$. The input/output signals of Δ can be bounded by an IQC. A precise definition is given below for an IQC in the time domain.

Definition 4. Let M be a symmetric matrix, i.e. $M = M^T \in \mathbb{R}^{n_z \times n_z}$ and Ψ a stable linear system, i.e. $\Psi \in \mathbb{RH}_\infty^{n_z \times (n_v + n_w)}$. A bounded, causal operator $\Delta : L_{2e}^{n_v} \to L_{2e}^{n_w}$ satisfies an IQC defined by (Ψ, M) if the following inequality holds for all $v \in L_2^{n_v}[0, \infty)$, $w = \Delta(v)$ and $T \geq 0$:

$$\int_0^T z(t)^T M z(t)\, dt \geq 0 \tag{6}$$

where z is the output of the linear system Ψ:

$$\begin{aligned} \dot{x}_\psi(t) &= A_\psi x_\psi(t) + B_{\psi 1} v(t) + B_{\psi 2} w(t), \;\; x_\psi(0) = 0 \\ z(t) &= C_\psi x_\psi(t) + D_{\psi 1} v(t) + D_{\psi 2} w(t) \end{aligned} \tag{7}$$

The notation $\Delta \in IQC(\Psi, M)$ is used if Δ satisfies the IQC defined by (Ψ, M).

Fig. 3 provides a graphic interpretation of the IQC. The input and output signals of Δ are filtered through Ψ. If $\Delta \in IQC(\Psi, M)$ then the output signal z satisfies the (time-domain) constraint in Equation (6) for any finite-horizon $T \geq 0$.

The proposed approach applies to the more general IQC framework introduced in [28] but with some technical restrictions. In particular, [28] provides a library of IQC multipliers that are satisfied by many important system components, e.g. saturation, time delay, and norm bounded uncertainty. The IQCs in [28] are expressed in the frequency domain as an integral constraint defined using a multiplier Π. The multiplier Π can be factorized as $\Pi =$

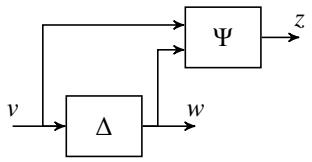

Figure 3. Graphic interpretation of the IQC

$\Psi^* M \Psi$ and this connects the frequency domain formulation to the time-domain formulation used in this paper. One technical point is that, in general, the time domain IQC constraint only holds over infinite horizons ($T = \infty$). The work in [23, 28] draws a distinction between hard/complete IQCs for which the integral constraint is valid over all finite time intervals and soft/conditional IQCs for which the integral constraint need not hold over finite time intervals. The formulation of an IQC in this paper as a finite-horizon (time-domain) inequality is thus valid for any frequency-domain IQC that admits a hard/complete factorization (Ψ, M). While this is somewhat restrictive, it has recently been shown in [23] and [32] that a wide class of IQCs have a hard factorization. The remainder of the paper will simply treat, without further comment, (Ψ, M) as the starting point for the definition of the finite-horizon IQC.

2. *Robustness Analysis of LPV Systems*

An uncertain LPV system is described by the interconnection of an LPV system G_ρ and an uncertainty Δ. This interconnection represents an upper linear fractional transformation (LFT), which is denoted $\mathcal{F}_u(G_\rho, \Delta)$. The uncertainty Δ is assumed to satisfy an IQC described by (Ψ, M). In the basic interconnection $\mathcal{F}_u(G_\rho, \Delta)$ the filter Ψ is included as shown in Fig. 4. For fixed Δ, $\|F_u(G_\rho, \Delta)\|$ will denote the largest L_2 gain over all allowable parameter trajectories:

$$\|F_u(G, \Delta)\| := \sup_{\substack{0 \neq d \in L_2^{n_d}[0,\infty) \\ \rho \in \mathcal{T},\ x_G(0)=0}} \frac{\|e\|_2}{\|d\|_2} \tag{8}$$

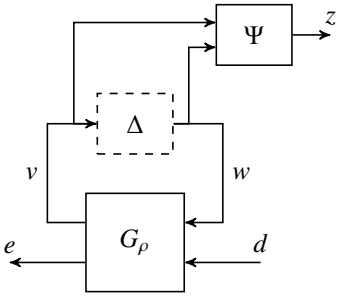

Figure 4. Analysis Interconnection

The dynamics of the interconnection in Fig. 4 depends on an extended LPV system of the form:

$$\begin{aligned} \dot{x} &= A(\rho)x + B_1(\rho)w + B_2(\rho)d \\ z &= C_1(\rho)x + D_{11}(\rho)w + D_{12}(\rho)d \\ e &= C_2(\rho)x + D_{21}(\rho)w + D_{22}(\rho)d, \end{aligned} \tag{9}$$

where the state vector is $x := \begin{bmatrix} x_G \\ x_\psi \end{bmatrix} \in \mathbb{R}^{n_G+n_\psi}$ with x_G and x_ψ denoting the state vectors of the LPV system G_ρ Equation (3) and the filter Ψ Equation (7), respectively. A dissipation inequality can be formulated to upper bound the worst-case L_2 gain of $\mathcal{F}_u(G_\rho, \Delta)$ (over all uncertainties) using the system Equation (9) and the time domain IQC Equation (6). This dissipation inequality is concretely expressed as a linear matrix inequality in the following theorem.

Theorem 2. Let Δ satisfy IQC(Ψ, M) and assume $F_u(G_\rho, \Delta)$ is well posed. Then $\|F_u(G_\rho, \Delta)\| \le \gamma$ if there exists a scalar $\lambda > 0$ and a continuously differentiable $P : \mathcal{P} \to \mathbb{R}^{n_x \times n_x}$ such that for all $(\rho, \dot{\rho}) \in \mathcal{P} \times \dot{\mathcal{P}}$: $P \ge 0$ and

$$\begin{bmatrix} PA + A^T P + \partial P & PB_1 & PB_2 \\ B_1^T P & 0 & 0 \\ B_2^T P & 0 & -I \end{bmatrix} + \lambda \begin{bmatrix} C_1^T \\ D_{11}^T \\ D_{12}^T \end{bmatrix} M \begin{bmatrix} C_1 & D_{11} & D_{12} \end{bmatrix} + \frac{1}{\gamma^2} \begin{bmatrix} C_2^T \\ D_{21}^T \\ D_{22}^T \end{bmatrix} \begin{bmatrix} C_2 & D_{21} & D_{22} \end{bmatrix} < 0 \tag{10}$$

In Equation (10) the dependency of the state space matrices on ρ has been omitted to shorten the notation.

Proof. The proof is based on defining a storage function $V : R^{n_x+n_\psi} \to \mathbb{R}^+$ by $V(x) = x^T P x$. Left and right multiply Equation (10) by $[x^T, w^T, d^T]$ and $[x^T, w^T, d^T]^T$ to show that V satisfies the dissipation inequality:

$$\lambda z(t)^T M z(t) + \dot{V}(t) \le \gamma^2 d(t)^T d(t) - e(t)^T e(t) \tag{11}$$

The dissipation inequality Equation (11) can be integrated from $t = 0$ to $t = T$ with the initial condition $x(0) = 0$ to yield:

$$\lambda \int_0^T z(t)^T M z(t)\, dt + V\left(x(T)\right) \le \gamma^2 \int_0^T d(t)^T d(t)\, dt - \int_0^T e(t)^T e(t)\, dt \tag{12}$$

It follows from the IQC condition Equation (6), $\lambda \ge 0$, and the non-negativity of the storage function V that

$$\int_0^T e(t)^T e(t)\, dt \le \gamma^2 \int_0^T d(t)^T d(t)\, dt \tag{13}$$

Hence $\|F_u(G, \Delta)\| \le \gamma$. □

A detailed proof of Theorem 2 as well as an extension to LPV systems with bounded parameter variation rates can be found in [5]. he connection of this theoretical result back to the robust closed-loop tracking (Figure 2) is briefly

summarized. The robust closed loop tracking specifies performance using a weight W. The feedback system also involves a scheduled controller K_ρ and an uncertain plant $F_u(G_\rho, \Delta)$. This robust tracking analysis problem can be rewritten in the form shown in Figure 4 with Δ "pulled out". The nominal part of the interconnection G_ρ contains the plant dynamics, scheduled controller, and performance weight. Thus the state x_G is the sum of the states of these three systems. The uncertainty Δ is described by IQCs Ψ which can have their own dynamics and state x_ψ. These states are purely used for the analysis and are not part of the implemented feedback system.

IV. Numerical Example

This section provides the analysis of a gain scheduled controller for a small unmanned aerial vehicle (UAV). The airframe is a commercial, off-the-shelf, radio-controlled aircraft called the Ultra Stick 120, as shown in Fig. 5. The University of Minnesota UAV Research Group has retrofitted the airframe with custom avionics for enabling research in the areas of real-time control, guidance, navigation, and fault detection [33]. The Ultra Stick 120 has a mass of 7.4 kg and a symmetrical airfoil wing spanning 1.92 m. It use conventional control surface configurations comprising a single vertical rudder with elevator, aileron, and flap surfaces. Each surface is independently actuated by a single electric, hobby-grade servo. The avionics include a sensor suite, a flight control computer, and a telemetry radio.

Before being given to University of Minnesota, this aircraft was originally used at NASA Langley Research Center where it was called FASER (Free-flying Aircraft for Subscale Experimental Research) [34]. A main advantage of this platform is that a high fidelity aerodynamics model is available. It is based on extensive static wind tunnel tests, which were later complemented with dynamic wind tunnel tests [35, 36]. The aerodynamic model is a nonlinear look-up table that includes effects due to the basic airframe, control surfaces, thrust, and angular rates.

Figure 5. Ultra Stick 120

The nominal, operational flight envelope is restricted in the $V - \alpha$ plane by $V \in [20, 26]$ m/s and $\alpha \in [0, 10]^\circ$. This flight envelope was identified in [37] by analyzing past flight test data gathered at University of Minnesota. For this nominal flight envelope a classical gain scheduled controller is designed. The aim of the study is to obtain the

permissible flight envelope for the aircraft with the designed controller using the approach detailed in Section II.B. The considered flight envelope is by far not exhaustive. In principle the flight envelope of the FASER has more complex shapes and includes additional scheduling parameters. There is no fundamental restriction in the proposed method in regard to analysing the complete flight envelope. The restriction on the $V - \alpha$ was chosen to keep the example illustrative.

The aircraft is trimmed over a grid of points ranging between $V \in [12, 36]$ m/s and $\alpha \in [-419]^\circ$. These bounds were chosen as they represent the area in the flight envelope at which a trim solution could still be found. At each trim point, Jacobian linearization is applied to obtain a linear system of the aircraft dynamics. These linearized models are then reduced to the classical short period approximation of the longitudinal motion flight dynamics. They only retain α and q as states.

A. Rate Command/Attitude Hold Controller

To demonstrate the effectiveness of the proposed LOC analysis, a simple classical gain scheduled controller was designed. The controller structure is a rate command/attitude hold type as shown in Fig. 6. It uses a proportional feedback of the angle of attack α and a proportional and integral feedback of the pitch rate error $q_c - q$. The controller is scheduled with airspeed V and angle of attack α. Hence the operating condition is specified by $\rho := [V, \alpha]^T$. The control input is the elevator δ_e.

$$\begin{aligned} \dot{x}_I &= q_c - q \\ \delta_e &= K_I(\rho)x_I + K_q(\rho)(q_c - q) + K_\alpha(\rho)\alpha \end{aligned} \tag{14}$$

The gains K_q and K_α were designed using pole placement at a grid of frozen parameter values that span the flight envelope. The desired frequency and damping of the short period mode were chosen as $\omega_{des} = 8$ rad/s and $\zeta_{des} = 0.7$, respectively. The integrator gain K_I is chosen such that the corresponding eigenvalue is at roughly -1 at each frozen parameter value.

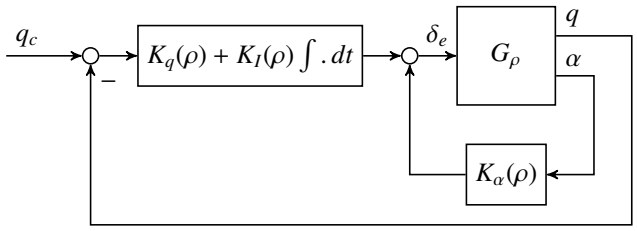

Figure 6. Rate Command/Attitude Hold Controller

B. Quantitative Loss of Control Analysis

In an initial analysis, the nominal LTI permissible flight envelope, see Definition 1, is computed. The bandwidth of the weighting filter for the tracking requirement is set to 1 rad/s, i.e.

$$W(s) = \frac{s+1}{2s+0.001}. \tag{15}$$

Using this weighting function, the maximum gain within the nominal flight envelope is 1. The results of this study are depicted in Fig. 7. The plot shows the nominal gain as a function of airspeed and angle of attack. The colorbar on the right of the subplot maps the nominal gain to the color shown the flight envelope. The black box in the figure indicates the nominal flight envelope for which the controller was designed. The dashed, red box is the permissible flight envelope based on the nominal LTI analysis. It is spanned by $V \in [14, 32]$ m/s and $\alpha \in [-2, 17]^\circ$. Note that the closed loop is unstable at low flight speeds and high angle of attacks (indicated by × in the figure).

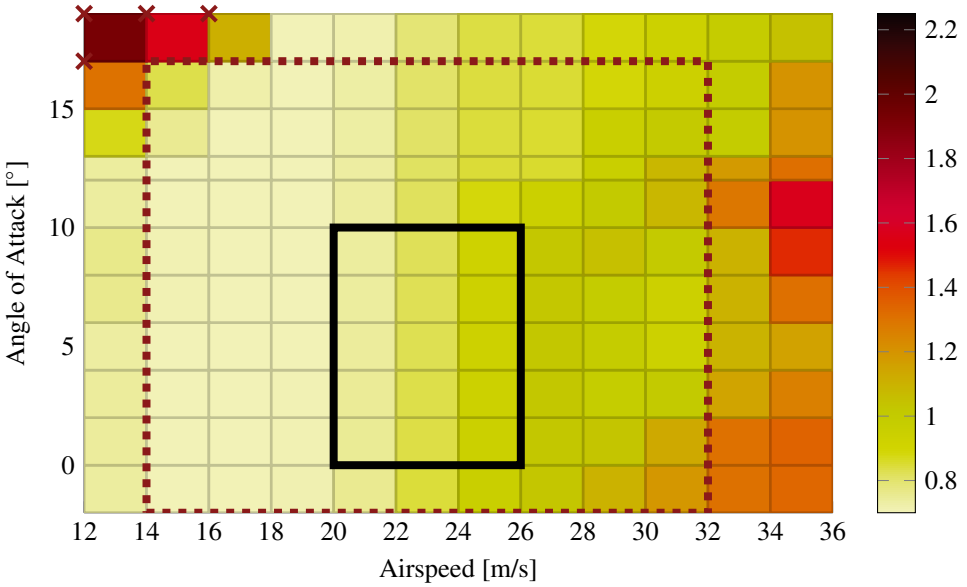

Figure 7. Tracking Performance over the Extended Flight Envelope

In the next analysis, model uncertainty is included. A ten percent multiplicative LTI uncertainty in the input of the plant is considered. The analysis is performed over the same grid of frozen values of ρ as the nominal one using the Matlab command `wcgain` as described in Section III. The results of the robust QLC analysis is given in Fig. 8. The robust permissible flight envelope is slightly smaller than the nominal one. It excludes higher airspeeds and is given by $V \in [14, 28]$ m/s and $\alpha \in [-2, 17]^\circ$.

Finally, both a nominal and robust LPV analysis are performed. Since the previous analyses only considered frozen parameter values, they do not capture the effects of the parameter variation. The parameter variation rates are bounded by $\left|\dot{V}\right| \leq 1\,\text{m/s}^2$ and $|\dot{\alpha}| \leq 40\,^\circ/\text{s}$. The parameter dependent storage function in Theorem 1 and Theorem 2 is specified as a second order polynomial function fo V and α, i.e. $P(V, \alpha) = P_1 + P_2\alpha + P_3 V + P_4\alpha^2 + P_5\alpha V + P_6 V^2$. Both LPV

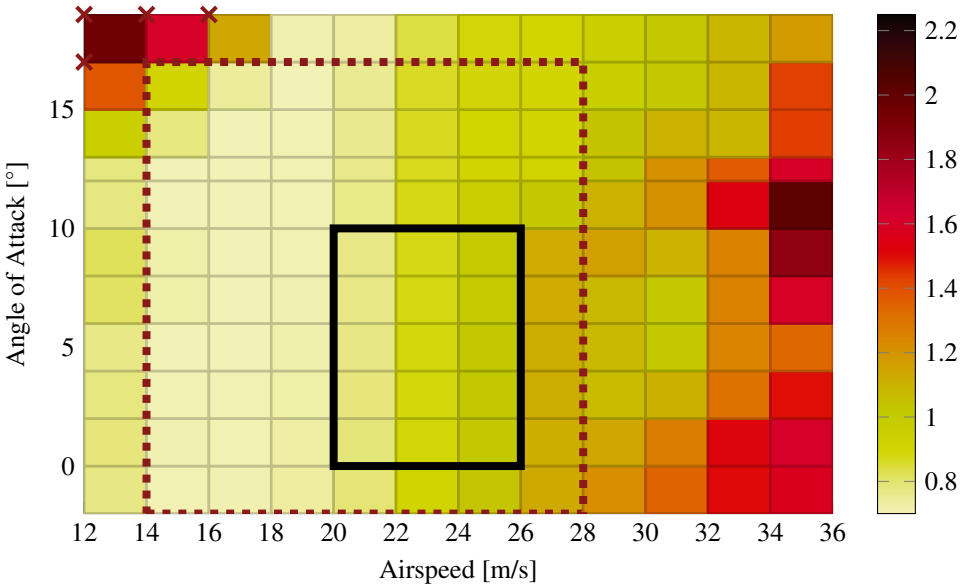

Figure 8. Robust Tracking Performance over the Extended Flight Envelope

analyses are used to assess the permissible envelopes of the nominal and robust LTI analysis respectively. Evaluation Theorem 1 over the permissible envelope of the nominal LTI analysis yields a nominal L_2 gain of 1.323. This is very close to the maximum frozen grid point LTI gain of 1.3. Hence, it is concluded that time variations in the operating point $\rho(t)$ has only a minor impact in this particular example.

The robust LPV analysis uses the same 10 percent multiplicative uncertainty as the LTI case. It is described by the two IQCs (Ψ_1, M_1) with $\Psi_1 = I$ and $M_1 = \left[\begin{smallmatrix} 0.1^2 & 0 \\ 0 & -1 \end{smallmatrix}\right]$ and (Ψ_2, M_2) with $\Psi_2 = \left[\begin{smallmatrix} \frac{1}{s+1} & 0 \\ 0 & \frac{1}{s+1} \end{smallmatrix}\right]$ and $M_2 = \left[\begin{smallmatrix} 0.1^2 & 0 \\ 0 & -1 \end{smallmatrix}\right]$. Using Theorem 2, a worst-case gain of 1.23 is obtained for the robust permissible envelope which again is less than the 1.3 that define the frozen point envelope. Note that the worst-case gain found by `wcgain` within the permissible envelope is 1.17 which is slightly lower than the LPV worst-case gain. The robust LPV analysis confirms the results of the nominal one that the time variations in the operating point in this particular example have little impact.

A key aspect of the proposed method is that it is very computationally efficient. The nominal flight envelope analysis took 0.5 seconds for the LTI analysis and 1.5 seconds for the LPV one. The robust flight envelope estimation is slightly more the demanding. The LTI and LPV robustness analysis took approximately 2 and 2.5 minutes respectively. All the results were obtained using a standard home office PC running Matlab.

The results of the robust permissible flight envelope analysis are validated using nonlinear simulation. In order to perform the simulation, the aircraft was trimmed at three different operating conditions, one within the nominal flight envelope, one within the permissible flight envelope and one outside. Norm-bounded dynamic LTI uncertainty (with a bound of 0.1) was introduced as a multiplicative uncertainty at the input to the elevator actuator. Monte Carlo simulations were performed by sampling this norm-bounded dynamic uncertainty using the `usample` function in Matlab (which itself calls `rssnb`). The algorithm effectively samples a random distribution of poles (up to 10

rad/sec) for the state matrix A. The input B and output C matrices are sampled from a normal distribution while the feedthrough matrix is assumed to be zero. The objective of the simulation was to track a doublet in the pitch rate. In the present example, 20 sample were used. The simulation results are presented in Figure 9 and Figure 10. In Figure 9, it can be seen that the control tracks well within the nominal flight envelope (–), as was expected. While there is some degradation in performance in the permissible flight envelope (–) it is anticipated that the pilot still has control of the aircraft. Outside the flight envelope (–), the tracking performance exhibits significant under and overshoot. Figure 10 shows the position of the aircraft within the different flight envelopes during the simulations.

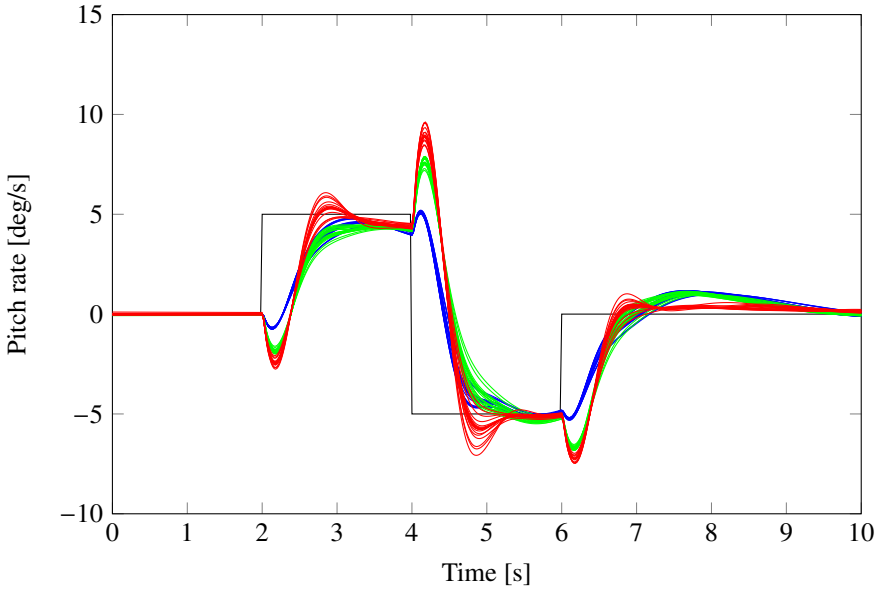

Figure 9. Robust tracking in the nonlinear simulation within the nominal flight envelope (–), the permissible flight envelope (–) and outside the flight envelope (–)

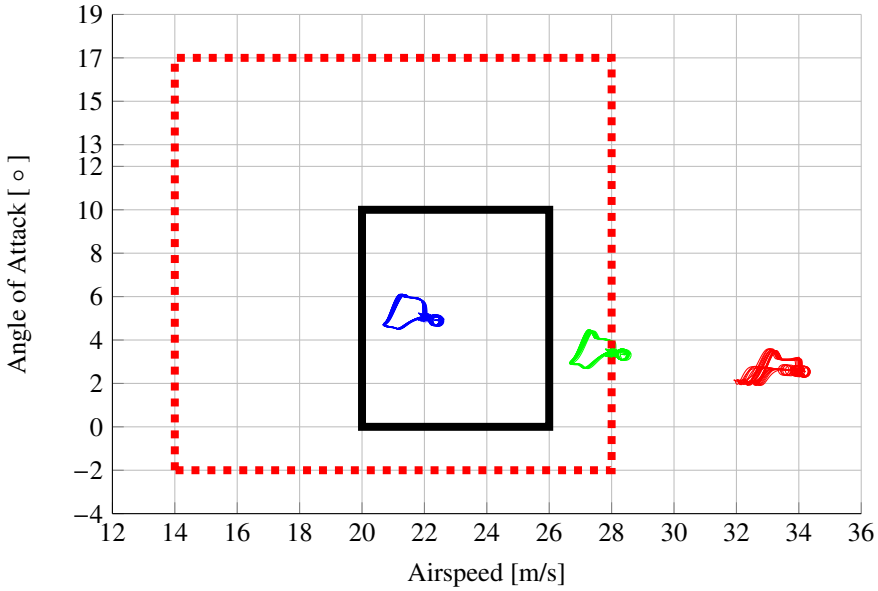

Figure 10. Trajectories of the nonlinear simulations in respect to the flight envelope

V. Conclusion

A metric to quantify the permissible flight envelope based on the closed-loop tracking performance has been proposed. The approach does not resort on extensive flight data. Inaccuracies in aircraft models are accounted for by adding uncertainty in the analysis. The approach can also handle LPV systems to describe the aircraft dynamics. Hence, it can account for time-varying dynamics as the aircraft transitions between different flight conditions. The effectiveness of the proposed method is demonstrated on the analysis of a classical gain scheduled controller for a small unmanned aerial vehicle, namely the Ultra Stick 120. The results show that it is important to include a robustness metric in the analysis. In the presented example, the parameter variation only has a minor influence. This can be expected, as the considered aircraft has very benign dynamics. It is still important to consider the time varying nature of the aircraft dynamics for loss of control, especially when analyzing high maneuverable aircraft.

Acknowledgments

This work was supported by the NASA Langley NRA Cooperative Agreement under Grant no. NNX12AM55A entitled "Analytical Validation Tools for Safety Critical Systems Under Loss-of-Control Conditions" Dr. Christine Belcastro is the technical monitor.

References

[1] Wilborn, J. E. and Foster, J. V., "Defining commercial transport loss-of-control: A quantitative approach," *AIAA Atmospheric Flight Mechanics Conference*, 2004, pp. AIAA 2004–4811, DOI 10.2514/6.2004-4811.

[2] Belcastro, C., "Validation of safety-critical systems for aircraft loss-of-control prevention and recovery," *AIAA Guidance, Navigation, and Control Conference*, 2012, pp. AIAA 2012–4987, DOI 10.2514/6.2012-4987.

[3] Boyd, S., Balakrishnan, V., and Kabamba, P., "A Bisection Method for Computing the H_∞ Norm of a Transfer Matrix and Related Problems," *Mathematics of Control, Signals, and Systems*, Vol. 2, 1989, pp. 207–219, DOI 10.1007/bf02551385.

[4] Packard, A., Balas, G., Liu, R., and Shin, J., "Results on Worst-Case Performance Assessment," *American Control Conference*, 2000, pp. 2425–2427, DOI 10.1109/acc.2000.878616.

[5] Pfifer, H. and Seiler, P., "Robustness Analysis of Linear Parameter Varying Systems Using Integral Quadratic Constraints," *International Journal of Robust and Nonlinear Control*, Vol. 25, 2014, pp. 2843 – 2864, DOI 10.1002/rnc.3240.

[6] Varga, A., Hansson, A., and Puyou, G., editors, *Optimization Based Clearance of Flight Control Laws, A Civil Aircraft Application*, Springer-Verlag, Heidelberg, 2012, DOI 10.1007/978-3-642-22627-4.

[7] Goman, M. G., Khramtsovsky, A. V., and Kolesnikov, E. N., "Evaluation of aircraft performance and maneuverability by computation of attainable equilibrium sets," *Journal of Guidance, Control, and Dynamics*, Vol. 31, No. 2, 2008, pp. 329–339.

[8] Kwatny, H. G., Dongmo, J.-E. T., Chang, B.-C., Bajpai, G., Yasar, M., and Belcastro, C., "Aircraft accident prevention: Loss-of-control analysis," *AIAA Guidance, Navigation, and Control Conference*, 2009, DOI 10.2514/6.2009-6256.

[9] Lygeros, J., "On reachability and minimum cost optimal control," *Automatica*, Vol. 40, No. 6, 2004, pp. 917–927.

[10] Pandita, R., Chakraborty, A., Seiler, P., and Balas, G., "Reachability and region of attraction analysis applied to GTM dynamic flight envelope assessment," *AIAA Guidance, Navigation, and Control Conference*, 2009, pp. 10–13.

[11] Lombaerts, T., Schuet, S. R., Wheeler, K., Acosta, D. M., and Kaneshige, J., "Safe maneuvering envelope estimation based on a physical approach," *AIAA Guidance, Navigation, and Control Conference*, American Institute of Aeronautics and Astronautics, 2013.

[12] Lombaerts, T., Schuet, S., Wheeler, K., Acosta, D., and Kaneshige, J., "Robust maneuvering envelope estimation based on reachability analysis in an optimal control formulation," *Conference on Control and Fault-Tolerant Systems*, IEEE, 2013, pp. 318–323.

[13] Mitchell, I. M., Bayen, A. M., and Tomlin, C. J., "A time-dependent Hamilton-Jacobi formulation of reachable sets for continuous dynamic games," *IEEE Transactions on automatic control*, Vol. 50, No. 7, 2005, pp. 947–957.

[14] Lichter, M., Bateman, A., and Balas, G., "Flight Test Evaluation of a Run-time Stability Margin Estimation Tool," *AIAA Guidance, Navigation, and Control Conference*, 2009, pp. AIAA 2009–6257, DOI 10.2514/6.2009-6257.

[15] Balas, G. J., Fialho, I., Packard, A., Renfrow, J., and Mullaney, C., "On the design of LPV controllers for the F-14 aircraft lateral-directional axis during powered approach," *American Control Conference*, Vol. 1, 1997, pp. 123–127.

[16] Papageorgiou, G., Glover, K., D'Mello, G., and Patel, Y., "Taking robust LPV control into flight on the VAAC Harrier," *IEEE Conference on Decision and Control*, Vol. 5, 2000, pp. 4558–4564.

[17] Belcastro, C. M., Khong, T. H., Shin, J.-Y., Kwatny, H., Chang, B.-C., and Balas, G. J., "Uncertainty modeling for robustness analysis of aircraft control upset prevention and recovery systems," *AIAA Conference on Guidance, Navigation and Control*, 2005.

[18] Russell, P. and Pardee, J., "JSAT Loss of Control: Results and Analysis, CAST Approved Final Report," Tech. rep., Commercial Aviation Safety Team, 2000.

[19] Jordan, T. and Bailey, R., "NASA Langley's AirSTAR Testbed: A Subscale Flight Test Capability for Flight Dynamics and Control System Experiments," *AIAA Guidance, Navigation, and Control Conference*, 2008, pp. AIAA 2008–6660, DOI 10.2514/6.2008-6660.

[20] Lombaerts, T., Huisman, H., Chu, P., Mulder, J. A., and Joosten, D., "Nonlinear reconfiguring flight control based on online physical model identification," *Journal of Guidance, Control, and Dynamics*, Vol. 32, No. 3, 2009, pp. 727–748.

[21] Skogestad, S. and Postlethwaite, I., *Multivariable Feedback Control*, John Wiley and Sons, Chichester, 2005.

[22] Zhou, K., Doyle, J., and Glover, K., *Robust and Optimal Control*, Prentice-Hall, New Jersey, 1996.

[23] Megretski, A., "KYP Lemma for Non-Strict Inequalities and the associated Minimax Theorem," arXiv, 2010.

[24] Balas, G., Chiang, R., Packard, A., and Safonov, M., "Robust Control Toolbox 3 User's Guide," Tech. rep., The Math Works, Inc., 2007.

[25] Hjartarson, A., Seiler, P. J., and Balas, G. J., "LPV Analysis of a Gain-Scheduled Control for an Aeroelastic Aircraft," *American Control Conference*, 2014, pp. 3778–3783, DOI 10.1109/acc.2014.6859301.

[26] Hjartarson, A., Packard, A., and Seiler, P., "LPVTools: A Toolbox for Modeling," *1st IFAC Workshop on Linear Parameter Varying Systems*, 2015.

[27] Bruinsma, N. and Steinbuch, M., "A fast algorithm to compute the H_∞ norm of a transfer function matrix," *Systems and Control Letters*, Vol. 14, 1990, pp. 287–293, DOI 10.1016/0167-6911(90)90049-z.

[28] Megretski, A. and Rantzer, A., "System Analysis via Integral Quadratic Constraints," *IEEE Trans. on Automatic Control*, Vol. 42, 1997, pp. 819–830, DOI 10.1109/9.587335.

[29] Wu, F., Yang, X. H., Packard, A., and Becker, G., "Induced $\mathcal{L}_2$ norm control for LPV systems with bounded parameter variation rates," *Int. Journal of Robust and Nonlinear Control*, Vol. 6, 1996, pp. 983–998.

[30] Scherer, C. and Wieland, S., "Linear Matrix Inequalities in Control," Lecture notes for a course of the Dutch institute of systems and control, Delft University of Technology, 2004.

[31] Balas, G., "Linear, parameter-varying control and its application to a turbofan engine," *Int. Journal of Robust and Nonlinear Control*, Vol. 12, 2002, pp. 763–796, DOI 10.1002/rnc.704.

[32] Seiler, P., "Stability Analysis with Dissipation Inequalities and Integral Quadratic Constraints," *IEEE Trans. on Automatic Control*, Vol. 60, 2015, pp. 1704–1709, DOI 10.1109/tac.2014.2361004.

[33] Dorobantu, A., Johnson, W., Lie, F. A., Taylor, B., Murch, A., Paw, Y. C., Gebre-Egziabher, D., and Balas, G., "An airborne experimental test platform: From theory to flight," *American Control Conference*, 2013, pp. 659–673, DOI 10.1109/acc.2013.6579912.

[34] Owens, D. B., Cox, D. E., and Morelli, E. A., "Development of a low-cost sub-scale aircraft for flight research: The FASER project," *25th AIAA Aerodynamic Measurement Technology and Ground Testing Conference*, No. 2006-3306, 2006, DOI 10.2514/6.2006-3306.

[35] Morelli, E. A. and DeLoach, R., "Wind tunnel database development using modern experiment design and multivariate orthogonal functions," *Proceedings of the 41st Aerospace Sciences Meeting and Exhibit. AIAA*, 2003, DOI 10.2514/6.2003-653.

[36] Hoe, G., Owens, B., and Denham, C., "Forced oscillation wind tunnel testing for faser flight research aircraft," *AIAA Atmospheric Flight Mechanics Conference*, 2012, DOI 10.2514/6.2012-4645.

[37] Freeman, P., *Reliability Assessment for Low-cost Unmanned Aerial Vehicles*, Ph.D. thesis, University of Minnesota, 2014.